Low Temperature Physics/Fizika Nizkikh Temperatur, 2021, vol. 47, No. 4, pp. 295–308

Magnetooscillations of temperature and microwave absorption in a highly correlated 2D electron gas on liquid helium

Yu. P. Monarkha

B. Verkin Institute for Low Temperature Physics and Engineering of the National Academy of Sciences of Ukraine
Kharkiv 61103, Ukraine
E-mail: monarkha@ilt.kharkov.ua

Received December 9, 2020, published online February 26, 2021

The Coulombic effect on microwave-induced electron heating in a 2D electron gas on liquid helium under quantizing magnetic field is theoretically studied. An extension of the linewidth of the intersubband resonance which takes into account squeezing of the electron density of states into Landau levels and strong internal electric fields of fluctuational origin is proposed. This approximation results in two-hump peaks of electron temperature and power absorption near certain values of the magnetic field. For low electron densities, the asymmetry of the two-hump peaks of power absorption is shown to be opposite to the asymmetry of electron temperature peaks, which explains experimental observations. The importance of two-ripplon emission processes for the description of subband occupancies and the energy relaxation rate was demonstrated.

Keywords: 2D electron gas, magnetooscillations, nonequilibrium phenomena, intersubband microwave absorption.

1. Introduction

The discovery of microwave-induced resistance oscillations (MIRO) and zero-resistance states (ZRS) in a high-mobility two-dimensional (2D) electron gas of semiconductor devices subjected to a perpendicular magnetic field [1–4] had inspired a large body of experimental and theoretical studies in various electron systems [5–7]. The effect of MIRO is caused by the microwave (MW) electric field whose polarization vector is directed along the plane of the 2D electron system (intrasubband excitation), though the actual mechanism responsible for this effect is still under debate (different theoretical mechanisms are reviewed in Ref. 8). In this case, resistance oscillations are observed for a quite arbitrary MW frequency $\omega > \omega_c$ (here ω_c is the cyclotron frequency), and ZRS appear in regions of oscillatory minima if MW power is high enough.

Similar MIRO and ZRS of different origin were observed in a nondegenerate 2D electron gas formed on the free surface of liquid helium [9, 10] when the two lowest subbands were tuned to the resonance with the MW frequency: $\omega_{2,1} \equiv (\Delta_2 - \Delta_1)/\hbar \to \omega$, where Δ_l (with $l = 1, 2, ...$) is the position of an energy level of an electron in the 1D potential well formed near the interface. The period of DC magnetoconductivity (σ_{xx}) oscillations is controlled only by the ratio $\omega_{2,1}/\omega_c$, and strong variations of σ_{xx} occur in the vicinity of magnetic field values B_m defined by the condition $\omega_{2,1}/\omega_c(B) = m$ (here $m = 1, 2, ...$). The theoretical explanation of this kind of MIRO is based on nonequilibrium electron population of the excited subband [11, 12] which triggers quasi-elastic intersubband scattering of electrons at helium vapor atoms and capillary-wave excitations (ripplons). Therefore, the presence of the vertical (out-of-plane) component of the MW electric field is important for observation of this effect. A remarkable property of the intersubband scattering is that it results in sign-changing corrections into electron magnetoconductivity σ_{xx} and even ZRS if the fractional occupancy of the excited subband $\bar{n}_2$ exceeds $\bar{n}_1 \cdot \exp(-\Delta_{2,1}/T_e)$, where $\bar{n}_1$ is the fractional occupancy of the ground subband, $\Delta_{2,1} = \Delta_2 - \Delta_1$, and T_e is the electron temperature. Therefore, an extra population of the second subband $\bar{n}_2$ caused by trivial heating of an electron gas cannot lead to sign-changing terms of the DC magnetoconductivity and ZRS. In order to observe this kind of MIRO in a degenerate electron system, the displacement from equilibrium should be such that electron distributions in two subbands can no longer be described by a single Fermi level [13].

Usually, quasi-elastic electron decay from the excited subband to the ground subband strongly heats the electron system because the energy $\Delta_{2,1}$ is transferred into the ki-

netic energy of electrons. In the absence of the magnetic field, the interplay between the MW excitation and the electron scattering by vapor atoms can heat electrons [14] up to about 10 K long before the quantum saturation is reached. If a perpendicular magnetic field is applied, the in-plane electron density of states is squeezed into a staircase of Landau levels which are broadened due to interaction with scatterers. In this case, quasi-elastic decay can be strongly suppressed if the staircases of Landau levels belonging to different subbands are not aligned, and the quantum saturation $\overline{n}_2 \to \overline{n}_1$ can be reached at rather low excitation rates. In the opposite regime, when the staircases of Landau levels are aligned ($\omega_{2,1}/\omega_c \to m$) electron system is heated due to quasi-elastic decay of electrons excited to the second subband by the MW. In other words, the electron temperature should also oscillate when varying $1/B$ with the period governed by the ratio $\omega_{2,1}/\omega_c$. The magnetooscillations of electron temperature were described previously [12] by a simple method which neglects electron-electron correlations and inelastic decay processes. At the same time, under experimental conditions the many-electron effect on intersubband MIRO was shown to be important even at rather low electron densities n_e on the order of $10^6\,\mathrm{cm}^{-2}$.

The many-electron theory of intersubband MIRO had explained [15, 16] a number of remarkable experimental observations (for a review, see Ref. 17). In spite of the good agreement between experimental data for conductivity extrema [18] and the respective theoretical predictions [15] formulated under the assumption $T_e = T$, there are some interesting effects observed which require further developments of the theory. For example, the first measurements [19] of intersubband absorption of MWs in surface electrons on liquid helium subjected to perpendicular magnetic field had revealed an unexpected feature: the strong suppression of absorption at magnetic fields B_m where the intersubband energy splitting $\Delta_{2,1}$ is a multiple number of the cyclotron energy $\hbar\omega_c$. This effect was not explained by the existing theories and requires additional studies. The same is valid for the hysteresis observed [20] in the dependence $\sigma_{xx}(B)$ near the conductivity minimum which is close to B_5. Electron heating and Coulombic effects are expected to be responsible for this feature.

There is another important point of the theory describing magnetooscillations induced by resonant intersubband excitation in a highly correlated 2D electron system. At low temperatures ($T \le 0.4$ K), the average kinetic energy of surface electrons T_e is much smaller than the average potential energy due to Coulomb interaction, and the conventional plasma parameter $\mathcal{P}_{\mathrm{pl}} = e^2\sqrt{\pi n_e}/T_e$ is much larger than unity even for rather small electron densities $n_e \gtrsim 10^6\,\mathrm{cm}^{-2}$. Therefore, in a wide range of this parameter, $10 < \mathcal{P}_{\mathrm{pl}} < 131$, surface electrons on liquid helium represent a highly correlated Coulomb liquid. Under equilibrium conditions ($T_e = T$) this problem was successfully solved employing the concept of quasi-uniform internal electric field E_f of fluctuational origin [21]. The typical value of the fluctuational electric field $E_f^{(0)} \simeq 3\sqrt{T_e}\,n_e^{3/4}$ depends on electron density and temperature T_e. In the presence of such a field, the dynamic structure factor (DSF) of the 2D electron liquid acquires an additional broadening of its maxima [22, 23] proportional to $\Gamma_f = \sqrt{2}eE_f^{(0)}\ell_B$ (here $\ell_B = \sqrt{\hbar c/eB}$ is the magnetic length) which affects strongly relaxation processes of electrons. The concept of quasi-uniform fluctuational electric field is valid if the plasma parameter $\mathcal{P}_{\mathrm{pl}} > 10$. With an increase of electron temperature induced by quasi-elastic electron decay processes the many-electron effect on relaxation rates increases ($\Gamma_f \propto \sqrt{T_e}$), but at the same time $\mathcal{P}_{\mathrm{pl}} \propto T_e^{-1}$ decreases and soon it can become smaller than 10. Actually it can even reach values on the order of unity, where the model of noninteracting electrons works quite well. Therefore, the many-electron theory of magnetooscillations should take this effect into account.

In this work, we present the theory of magnetooscillations of temperature and MW absorption of surface electrons on liquid helium which takes into account changes in the many-electron effect caused by electron heating as well as the specific nature of inelastic relaxation processes [24, 25] in this system. We shall modify the model describing the linewidth of the intersubband resonance, for it to be applicable for highly correlated electrons under a quantizing magnetic field. This modification and the internal forces affect strongly the shape of magnetooscillations. We shall demonstrate that intersubband MW absorption generally is not an increasing function of the electron temperature, as it is in usual intrasubband experiments, and, therefore, the asymmetry of electron temperature peaks in most cases is not the same as the asymmetry of power absorption peaks which explains experimental observations.

2. Intersubband transition rates under magnetic field

Consider a 2D electron gas formed on a flat substrate of liquid helium. In a 2D system, an electron subjected to a moderately-strong perpendicular magnetic field has a discrete energy spectrum called the staircase of Landau levels:

$$\varepsilon_n = \hbar\omega_c\left(n + 1/2\right),\ n = 0, 1, 2, \ldots \tag{1}$$

Each Landau level is degenerate (ε_n is independent of the center coordinate quantum number X); the degeneracy of a level is given by $S_A/2\pi\ell_B^2$, where S_A is the surface area. Therefore, interaction with scatterers broadens Landau levels. For short-range scatterers, like helium vapor atoms, the collision broadening [26]

$$\Gamma_n \equiv \Gamma = \sqrt{\frac{2}{\pi}\hbar^2\omega_c\nu_0} \tag{2}$$

is independent of the level number n; here ν_0 is the momentum relaxation rate for $B = 0$. This property is very convenient for studying nonequilibrium phenomena with $T_e \gtrsim \hbar\omega_c$.

In the self-consistent Born approximation [26] (SCBA), the density of states of Landau levels has the semi-elliptical shape. The cumulant approach gives the Gaussian shape [27]

$$-\mathrm{Im}G_n(\varepsilon) = \frac{\sqrt{2\pi}\hbar}{\Gamma_n}\exp\left[-\frac{2(\varepsilon-\varepsilon_n)^2}{\Gamma_n^2}\right]$$

[here $G_n(\varepsilon)$ is the single-electron Green's function] which is more suitable for lower levels, and more convenient for analytical evaluations. Therefore, it also is often employed for calculation various relaxation rates caused by scatterers in the way the semi-elliptical shape is used in the SCBA theory: effects of scattering are described in the lowest Born approximation, while the effect of broadening of the density of states is considered using the Green's-function formalism.

When describing properties of a photo-excited 2D electron gas, the excited subbands should be included in the consideration. In this case, the electron energy spectrum is given by $\mathcal{E}_{l,n} = \Delta_l + \varepsilon_n$, and the collision broadening of Landau levels becomes dependent on the subband number: $\Gamma_{l,n}$. If electron heating is not too strong ($T_e \lesssim 3$ K), one can restrict the consideration by two subbands: the ground ($l = 1$) and the first excited ($l = 2$). At stronger heating, the population of higher subbands should be taken into account. In this paper, we shall mostly consider the two-subband model described by fractional occupancies $\bar{n}_l = N_l / N_e$, where N_e is the total number of surface electrons. The subband occupancies are determined by the rate equation which includes the stimulated absorption (emission) rate r_{mw} and the transition rates between the subbands $\bar{\nu}_{l\to l'}$ caused by scattering at vapor atoms and ripplons.

The interaction Hamiltonian describing electron scattering by vapor atoms usually has a very simple form

$$H_{\mathrm{int}}^{(a)} = V^{(a)}\sum_a \delta(\mathbf{R}_e - \mathbf{R}_a), \quad V^{(a)} = \frac{2\pi\hbar^2\zeta_s}{m_e}, \qquad (3)$$

where ζ_s is the effective scattering length, $\mathbf{R}_e$ and $\mathbf{R}_a$ are the 3D radius-vectors describing positions of an electron and a vapor atom respectively. This point together with the result of Eq. (2) makes it attractive to study electron heating and the many-electron effect in the vapor atom scattering regime, when quasi-elastic electron scattering by ripplons can be neglected. For liquid ^{3}He, this condition is realized at $T \geq 0.4$ K. Then, the pure ripplon scattering regime ($T \simeq 0.2$ K) can be modeled by choosing the proper values for Γ and r_{mw}. It should be noted that even in the vapor atom scattering regime one cannot neglect inelastic electron scattering by pairs of energetic ripplons caused by nonlinear terms in the interaction Hamiltonian [24, 25].

For the highly correlated multisubband 2D electron system, it is very useful to describe [12, 15] electron scattering in terms of the dynamic structure factor (DSF) of the electron liquid $S_{l,l'}(q,\omega)$. This allows us to collect correctly contributions from different scattering processes using the basic property of the DSF as a function of the frequency argument. In this method, following the ideas of the SCBA, difficulties of divergence caused by the singular nature of the density of states in 2D electron systems can be avoided by the replacement

$$\delta(\varepsilon-\varepsilon_n) \to -\frac{1}{\pi\hbar}\mathrm{Im}G_{l,n}(\varepsilon)$$

which takes into account the broadening of Landau levels at each subband. In these terms, the intersubband transition rate can be found as [12, 15]

$$\bar{\nu}_{l\to l'}^{(a)} = \frac{\hbar\nu_0^{(a)}}{m_e S_A} p_{l,l'}\sum_{\mathbf{q}} S_{l,l'}(q,\omega_{l,l'}), \qquad (4)$$

where $\omega_{l,l'} = (\Delta_l - \Delta_{l'})/\hbar$,

$$\nu_0^{(a)} = \frac{m_e n_a^{(3\mathrm{D})}(V^{(a)})^2}{\hbar^3 B_{1,1}}, \quad p_{l,l'} = \frac{B_{1,1}}{B_{l,l'}}, \qquad (5)$$

$$\frac{1}{B_{l,l'}} = \frac{1}{L_z}\sum_{k_z}\left|\left(\mathrm{e}^{ik_z z}\right)_{l',l}\right|^2, \qquad (6)$$

$n_a^{(3\mathrm{D})}$ is the density of vapor atoms, $\mathbf{Q} \equiv (\mathbf{q}, k_z)$ is the momentum exchange at a collision, and L_z is the "box" size in z-direction. The subscript indexes l and l' in the DSF of the multisubband 2D electron system ($S_{l,l'}$) indicate that the level broadening depends on l. For vapor atom scattering described by Eq. (3), we have $\Gamma_l = \sqrt{p_{l,l}}\,\Gamma_1$, where Γ_1 is given by Eq. (2).

For noninteracting electrons, the DSF of the multisubband nondegenerate system is defined as [12]

$$S_{l,l'}(q,\Omega) = \frac{2}{\pi\hbar Z_{\|}}\sum_{n,n'}\int d\varepsilon \mathrm{e}^{-\varepsilon/T_e} I_{n,n'}^2(x_q)\times$$

$$\times\, \mathrm{Im}G_{l,n}(\varepsilon)\mathrm{Im}G_{l',n'}(\varepsilon+\hbar\Omega), \qquad (7)$$

where $Z_{\|} = \sum_n \exp(-\varepsilon_n/T_e)$,

$$I_{n,n'}^2(x) = \frac{[\min(n,n')]!}{[\max(n,n')]!}x^{|n-n'|}\mathrm{e}^{-x}\left[L_{\min(n,n')}^{|n-n'|}(x)\right]^2, \qquad (8)$$

$x_q = q^2\ell_B^2/2$, and $L_n^m(x)$ are the associated Laguerre polynomials. The frequency argument of the DSF is denoted here by the capital letter Ω to avoid confusing it with the MW frequency ω. The detailed balance of intersubband transition rates given by Eq. (4), $\bar{\nu}_{l'\to l} = \exp(-\Delta_{l,l'}/T_e)\bar{\nu}_{l\to l'}$, follows directly from the basic property of the equilibrium DSF:

$$S_{l,l'}(q,-\Omega) = \exp\left(-\frac{\hbar\Omega}{T_e}\right)S_{l',l}(q,\Omega). \qquad (9)$$

For degenerate electron system, the definition of the DSF and its basic property was given in Ref. 13.

From Eqs. (4) and (7) it is quite clear that the decay rate $\overline{\nu}^{(a)}_{2\to1}$ should have sharp maxima when $(n'-n)\omega_c \to \omega_{2,1}$. Under usual conditions, the system of surface electrons on liquid helium is characterized by extremely narrow Landau levels: $\Gamma_{l,n} \ll T, \hbar\omega_c$. Therefore, the decay rate caused by quasi-elastic scattering is exponentially small if Landau levels of the two subbands are out of alignment (B substantially differs from B_m).

For highly correlated electrons, the many-electron theory of intersubband scattering is based on employment of the DSF of the Coulomb liquid which can be found by proper averaging over the quasi-uniform fluctuational electric field E_f and comparing the final result with the DSF of the 2D Wigner solid [23]. The outcome is that instead of Eq. (7) one should use the following many-electron form of the DSF

$$S^{(\mathrm{ME})}_{l,l'}(q,\Omega) = \frac{2\sqrt{\pi}\hbar}{Z_\parallel}\sum_{n,n'}\frac{I^2_{n,n'}(x_q)}{\sqrt{\Gamma^2_{l,n;l',n'}+x_q\Gamma^2_C}}\mathrm{e}^{-\varepsilon_n/T_e}\times$$

$$\times\exp\left\{-\frac{\left[\hbar\Omega - m\hbar\omega_c - (\Gamma^2_{l,n}+x_q\Gamma^2_C)/4T_e\right]^2}{\Gamma^2_{l,n;l',n'}+x_q\Gamma^2_C}\right\}, \quad (10)$$

where $m = n'-n$, $\Gamma^2_{l,n;l',n'} = (\Gamma^2_{l,n}+\Gamma^2_{l',n'})/2$ is the average broadening, $\Gamma_C = \Gamma_f \equiv \sqrt{2}eE^{(0)}_f\ell_B$ and we had neglected a small term $\Gamma^2_{l,n}/8T^2_e$ in the argument of the exponential function. Thus, strong quasi-uniform internal forces can induce a substantial broadening of the DSF and the peaks of the decay rate $\overline{\nu}^{(a)}_{2\to1}(B)$. It should be noted that the correction $x_q\Gamma^2_C$ in the Gaussian form of Eq. (10) cannot be attributed to the broadening of Landau levels, because a quasi-uniform electric field can be eliminated by a proper choice of the reference frame [22, 23] and the correction depends on the momentum exchange at a collision q entering the dimensionless parameter x_q. In the following, we shall omit the superscript (ME) of the DSF of the multi-subband 2D Coulomb liquid remembering that the single-electron form can be obtained by fixing Γ_C to zero.

As noted in the Introduction, the concept of quasi-uniform fluctuational electric field and the relationship $\Gamma_C = \Gamma_f$ are valid only for large values of the plasma parameter $\mathcal{P}_{\mathrm{pl}} \geq 10$, and they fail if electron heating makes $\mathcal{P}_{\mathrm{pl}}$ smaller than 10. At present, there are no a many-electron theory describing the electron system in the range $1 < \mathcal{P}_{\mathrm{pl}} < 10$, therefore we shall construct a simple interpolation model. First, we note that in ordinary metals, where the average Coulomb interaction energy and quantum kinetic energy are on the same order of magnitude, the model of free quasiparticles well describes major transport properties. Therefore, it is reasonable to assume that the Coulomb broadening Γ_C should vanish at $\mathcal{P}_{\mathrm{pl}} \to 1$ which would transform the DSF of Eq. (10) into the result of the single-electron theory. Then, we can assume that the effect of the Coulomb broadening as a function of $\mathcal{P}_{\mathrm{pl}}$ gradually reduces in the region $1 < \mathcal{P}_{\mathrm{pl}} < 10$ and approximate this reduction by a simple interpolation form

$$\Gamma_C = \Gamma_f \tanh\left(\frac{\mathcal{P}_{\mathrm{pl}}-1}{5}\right)\theta\left(\mathcal{P}_{\mathrm{pl}}-1\right), \quad (11)$$

where $\theta(x) = 1$ if $x \geq 0$ and $\theta(x) = 0$ otherwise (the Heaviside step function). For this approximation, Γ_C is only 5 % smaller than Γ_f at $\mathcal{P}_{\mathrm{pl}} = 10$, and, as a function of T_e, it smoothly vanishes when $\mathcal{P}_{\mathrm{pl}}(T_e) \to 1$. We expect that at low electron densities $n_e \sim 10^6\,\mathrm{cm}^{-2}$ the approximation of Eq. (11) will describe the effect of electron heating much better than the assumption $\Gamma_C = \Gamma_f$ and a rough step-function approximation: $\Gamma_C \simeq \Gamma_f \times \theta(\mathcal{P}_{\mathrm{pl}} - 10)$.

Beyond the regions of $\overline{\nu}^{(a)}_{2\to1}$ peaks, the decay rate caused by inelastic two-ripplon (2R) scattering processes [25] becomes larger than $\overline{\nu}^{(a)}_{2\to1}$. Therefore, these processes should be included into the rate equation for fractional occupancies $\overline{n}_l$. The 2R scattering originates from nonlinear terms in the electron-ripplon interaction Hamiltonian

$$H^{(2\mathrm{R})}_{\mathrm{int}} = \frac{1}{S_A}\sum_{\mathbf{q},\mathbf{q}'}W_{\mathbf{q},\mathbf{q}'}(z)\xi_{\mathbf{q}}\xi_{\mathbf{q}'}\exp\left[i(\mathbf{q}+\mathbf{q}')\cdot\mathbf{r}\right], \quad (12)$$

here $\xi_{\mathbf{q}} = Q_q(b_{\mathbf{q}} + b^\dagger_{-\mathbf{q}})$, $Q_q = \sqrt{\hbar q/2\rho\omega_q}$, $\omega_q \simeq \sqrt{\alpha/\rho}q^{3/2}$ is the spectrum of capillary waves, α and ρ are the surface tension and mass density of liquid helium, respectively, $b^\dagger_{-\mathbf{q}}$ and $b_{\mathbf{q}}$ are the creation and destruction operators of ripplons. The coupling function $W_{\mathbf{q},\mathbf{q}'}(z)$ generally has a very complicated form. It can be simplified by taking into account that the matrix elements of $\langle n, X|\exp[i(\mathbf{q}+\mathbf{q}')\cdot\mathbf{r}]|n', X'\rangle$ are proportional to the factor $\exp[-(\mathbf{q}+\mathbf{q}')^2\ell^2_B/4]$ which means that inelastic 2R scattering by short-wavelength excitations ($q \gg \ell^{-1}_B$) is possible only if $\mathbf{q}' \approx -\mathbf{q}$. In this case, one can replace $W_{\mathbf{q},\mathbf{q}'}(z)$ with a new function $W_q(z)$ depending only on the absolute value q and on the parameters of the 1D potential well near the interface: $U_e(z) = V_0 + \mathrm{v}(z)$, where $\mathrm{v}(z) = -\Lambda/z + eE_\perp z$, the potential barrier at the liquid surface $V_0 \approx 1\,\mathrm{eV}$, the parameter of the image potential Λ depends on the dielectric constant of liquid helium in the usual way, and $E_\perp$ is the pressing electric field.

The matrix elements $(W_q)_{l,l'}$ were found only for two limiting cases $q > q_*$ and $q < q_*$, where $q_* \simeq 2\sqrt{\varkappa_0\gamma} \approx \approx 1.5\cdot10^7\,\mathrm{cm}^{-1}$, the parameter $\gamma^{-1} \approx 100$ Å describes electron localization length in the 1D potential well above the

surface, and $\varkappa_0^{-1} = \hbar/\sqrt{2m_e V_0} \approx 2$ Å is the penetration length of the electron wavefunction into the liquid phase. In the intermediate case, an interpolation based on the simple joining of the asymptotes was used [25]. In this work, we shall use a smooth interpolation which does not use the parameter q_*:

$$\left(W_q\right)_{l,l'} = W_{l,l'}^{(\mathrm{sh})} \tanh\left[\frac{q^2}{W_{l,l'}^{(\mathrm{sh})}}\left(\frac{p_z^2}{2m_e}\right)_{l,l'}\right], \qquad (13)$$

where p_z is the electron momentum, and $W_{l,l'}^{(\mathrm{sh})}$ is the short-wavelength asymptote independent of q:

$$W_{l,l'}^{(\mathrm{sh})} = \varkappa_0\sqrt{\left(\frac{\partial \mathrm{v}}{\partial z}\right)_{l,l}\left(\frac{\partial \mathrm{v}}{\partial z}\right)_{l',l'}}\,. \qquad (14)$$

The interpolation of Eq. (13) as a function of q is shown in Fig. 1 by solid lines. The previously used interpolation [25] is shown by dashed lines. Obviously, the smooth form of Eq. (13) will reduce a little bit the contribution of 2R scattering into the decay rate and energy relaxation rate as compared to the simple combined form based on joining of the asymptotes. In our numerical evaluations, here and below we consider liquid ^{3}He as a substrate for surface electrons.

The 2R scattering is substantially inelastic. Therefore, the broadening of Landau levels is unimportant for calculation of scattering probabilities. The many-electron effect can also be neglected if $\Gamma_C \ll \hbar\omega_c$. Assuming that the capillary wave spectrum $\omega_q \propto q^{3/2}$ remains to be valid in the short-wavelength range as well, and using the lowest Born approximation, one can find the decay rate caused by 2R emission processes

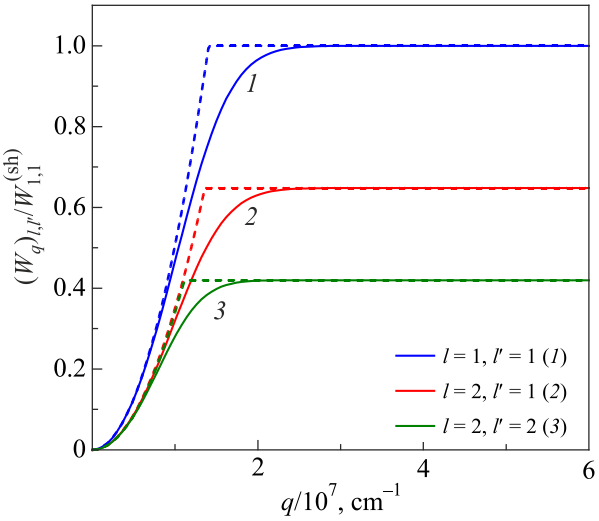

Fig. 1. (Color online) Illustration of two interpolations used for describing matrix elements of the two-ripplon coupling function $(W_q)_{l,l'}$: the smooth form of Eq. (13) (solid lines), the simple joining of the asymptotes used previously [25] (dashed lines).

$$\bar{\nu}_{2\to1}^{(\mathrm{2R,em})} = \frac{1}{12\pi\alpha^{3/2}\rho^{1/2}\ell_B^2}\sum_n \frac{\mathrm{e}^{-\varepsilon_n/T_e}}{Z_\parallel}\times$$

$$\times\sum_{n'}\left\{(W_q)_{2,1}^2\frac{(\mathcal{N}_q+1)^2}{q^{1/2}}\right\}_{q=q_m^{(\mathrm{em})}}, \qquad (15)$$

where $m = n' - n$, $\mathcal{N}_q$ is the distribution function of ripplons, and

$$q_m^{(\mathrm{em})} = \left(\frac{\rho}{4\alpha}\right)^{1/3}\left(\omega_{2,1} - m\omega_c\right)^{2/3}\theta\left(\omega_{2,1} - m\omega_c\right). \qquad (16)$$

In the sum of Eq. (15), the actual number m is restricted by the condition $m < \omega_{2,1}/\omega_c$. As compared to the previously found result [25], here we include higher Landau levels of the excited subband because of electron heating. According to Eqs. (15) and (16), the decay rate $\bar{\nu}_{2\to1}^{(\mathrm{2R,em})}$ oscillates with $1/B$, but in contrast with elastic decay it has small minima at the level alignment condition $\omega_{2,1} - m\omega_c = 0$. The more important point is that $\bar{\nu}_{2\to1}^{(\mathrm{2R,em})}$ slowly varies in between the characteristic values B_m remaining to be about $1.6\cdot10^6$ s^{-1}. It should be noted that recent experimental studies [28] of electron decay are in good (even numerical) agreement with the result of the theory based on 2R emission processes [25].

Electron scattering down to the ground subband can be also caused by absorption 2R processes. In this case, the energy conservation yields the following wave-vectors of ripplons

$$q_m^{(\mathrm{ab})} = \left(\frac{\rho}{4\alpha}\right)^{1/3}\left(m\omega_c - \omega_{2,1}\right)^{2/3}\theta\left(m\omega_c - \omega_{2,1}\right), \qquad (17)$$

where $m = n' - n$ should be positive and large enough. The corresponding contribution into the decay rate is found as

$$\bar{\nu}_{2\to1}^{(\mathrm{2R,ab})} = \frac{1}{12\pi\alpha^{3/2}\rho^{1/2}\ell_B^2}\sum_n \frac{\mathrm{e}^{-\varepsilon_n/T_e}}{Z_\parallel}\times$$

$$\times\sum_{n'}\left\{(W_q)_{2,1}^2\frac{(\mathcal{N}_q)^2}{q^{1/2}}\right\}_{q=q_m^{(\mathrm{ab})}}. \qquad (18)$$

Since the lowest value of m in $q_m^{(\mathrm{ab})}$ is independent of n, the contribution $\bar{\nu}_{2\to1}^{(\mathrm{2R,ab})}$ is independent of T_e. The full decay rate $\bar{\nu}_{2\to1}^{(\mathrm{2R})} = \bar{\nu}_{2\to1}^{(\mathrm{2R,em})} + \bar{\nu}_{2\to1}^{(\mathrm{2R,ab})}$ is shown in Fig. 2 by the solid line calculated for the fixed electron temperature $T_e = T = 0.4$ K. The dashed line indicates the contribution from emission processes only $\bar{\nu}_{2\to1}^{(\mathrm{2R,em})}$.

The reverse transition rate $\bar{\nu}_{1\to2}^{(\mathrm{2R,ab})}$ caused by 2R absorption processes depends strongly on the electron temperature. It has the form given in the right side of Eq. (18) where $q_m^{(\mathrm{ab})}$ should be substituted with $q_{-m}^{(\mathrm{em})}$ which take into account that absorption 2R scattering occurs from a

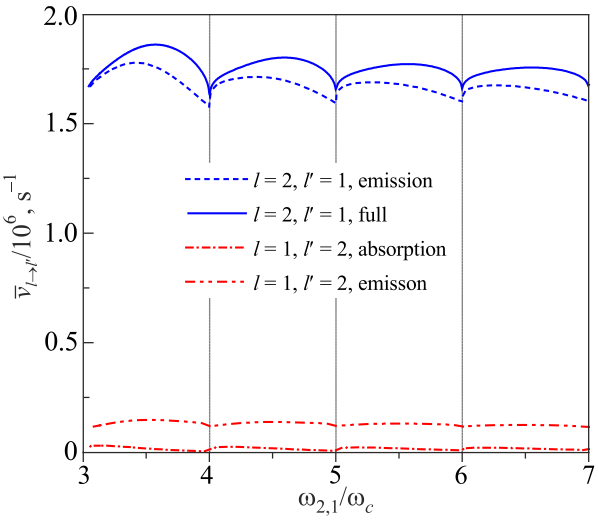

Fig. 2. (Color online) Two-ripplon scattering transition rates versus the ratio $\omega_{2,1}/\omega_c(B)$: the decay rate $2\to 1$ at $T_e = T = 0.4$ K (blue lines: emission — dashed, full contribution — solid), the rate of reverse scattering $1\to 2$ at $T_e = 3$ K (red lines: absorption — dash-dotted line, emission — dash-dot-dotted line).

state ($l = 1$, n) to a state ($l' = 2$, n') and in Eq. (16) the sign of m should be changed to the opposite. In this case, the lowest value of m depends on n and can be negative. It is quite obvious that at equilibrium, when $T_e = T$, the contributions $\bar{\nu}^{(2R,ab)}_{1\to 2}$ and $\bar{\nu}^{(2R,em)}_{2\to 1}$ satisfy the detail balance condition. For heated electrons, this relationship is not valid.

In a similar way, one can consider reverse transitions caused by 2R emission $\bar{\nu}^{(2R,em)}_{1\to 2}$ which become substantial only at strong electron heating $T_e \sim 3$ K. Obviously, $\bar{\nu}^{(2R,em)}_{1\to 2}$ has the form given in the right side of Eq. (15) where $q^{(em)}_m$ should be substituted with $q^{(ab)}_{-m}$ which take into account that emission 2R scattering occurs from a state ($l = 1$, n) to a state ($l' = 2, n'$) and in Eq. (17) the sign of m should be changed to the opposite. At equilibrium ($T_e = T$), the contributions $\bar{\nu}^{(2R,em)}_{1\to 2}$ and $\bar{\nu}^{(2R,ab)}_{2\to 1}$ satisfy the detail balance condition which fails if $T_e > T$. The contributions $\bar{\nu}^{(2R,ab)}_{1\to 2}$ and $\bar{\nu}^{(2R,em)}_{1\to 2}$ calculated for $T_e = 3$ K are shown in Fig. 2 by the red dash-dotted and dash-dot-dotted line respectively. The full rate of the reverse scattering $\bar{\nu}^{(2R)}_{1\to 2} = \bar{\nu}^{(2R,ab)}_{1\to 2} + \bar{\nu}^{(2R,em)}_{1\to 2}$ will be included in the rate equation for fractional occupancies of two lowest subbands.

It should be emphasized that for numerical calculations the sums over n and n' entering Eqs. (15) and (18) can be changed into more convenient sums over n and m which greatly reduces the evaluation time in spite of their cumbersome analytical expressions.

3. Subband occupancies

In this work, we shall assume that the MW stimulated absorption (emission) rate r_{mw} and the electron temperature are not too high ($T_e \lesssim 3$ K), so that we can neglect electron population of higher subbands with $l > 2$. In this case, the two-subband model can be considered as a good approximation for obtaining fractional occupancies $\bar{n}_1$ and $\bar{n}_2$. Using definitions given in the previous Section, the rate equation can be written as

$$r_{mw}\left(\bar{n}_1 - \bar{n}_2\right) = \bar{\nu}^{(a)}_{2\to 1}\left(\bar{n}_2 - e^{-\Delta_{2,1}/T_e}\bar{n}_1\right) + \\ + \bar{\nu}^{(2R)}_{2\to 1}\bar{n}_2 - \bar{\nu}^{(2R)}_{1\to 2}\bar{n}_1, \qquad (19)$$

and the relative occupancy

$$\eta \equiv \frac{\bar{n}_2}{\bar{n}_1} = \frac{r_{mw} + \bar{\nu}^{(a)}_{2\to 1}e^{-\Delta_{2,1}/T_e} + \bar{\nu}^{(2R)}_{1\to 2}}{r_{mw} + \bar{\nu}^{(a)}_{2\to 1} + \bar{\nu}^{(2R)}_{2\to 1}} \qquad (20)$$

saturates ($\eta \to 1$, $\bar{n}_2 \to \bar{n}_1$) when $r_{mw} \gg \bar{\nu}^{(a)}_{2\to 1} + \bar{\nu}^{(2R)}_{2\to 1}$. At small excitation rates, when r_{mw} can be neglected in Eq. (20), η is equal to the usual Boltzmann factor. The fractional occupancies are found as $\bar{n}_1 = (1+\eta)^{-1}$ and $\bar{n}_2 = 1 - \bar{n}_1$.

A very important point concerns the dependence of r_{mw} on the magnetic field. The MW excitation rate has the usual resonant form

$$r_{mw} = \frac{1}{2}\frac{\Omega_R^2\gamma_{opt}}{\left(\omega - \omega_{2,1}\right)^2 + \gamma^2_{opt}}, \qquad (21)$$

where γ_{opt} is the linewidth, Ω_R is the Rabi frequency given by $\hbar\Omega_R = eE_{mw}\langle 2|z|1\rangle$, and E_{mw} is the MW field. Scatterers and the inhomogeneous pressing electric field contribute into γ_{opt}. In experiments [10], the inhomogeneous broadening $\gamma_{inh} \simeq 9.4\cdot 10^8\,\mathrm{s}^{-1}$. The contribution of vapor atom scattering into the linewidth $\gamma^{(a)}_{opt}$ was calculated previously [29] only for the case of zero magnetic field. Under these conditions, γ_{inh} is substantially larger than $\gamma^{(a)}_{opt}$ in the low temperature regime ($T \lesssim 0.4$ K). In the presence of a quantizing magnetic filed, an enhancement factor $\hbar\omega_c/\sqrt{\pi}\Gamma_{l,n}$ should increase the contribution of electron scattering into the linewidth [12]. It should be noted that we can neglect the contribution of 2R scattering into γ_{opt} because γ_{inh} and $\gamma^{(a)}_{opt}$ (at $T \geq 0.4$ K) are about three orders of magnitude larger. At the same time, one should keep $\bar{\nu}^{(2R)}_{2\to 1}$ in the rate equation and in Eq. (20) because $\bar{\nu}^{(2R)}_{2\to 1}$ can be on the same order of magnitude as r_{mw}.

The effect of a perpendicular magnetic field and the internal fluctuational electric field on $\gamma^{(a)}_{opt}$ can be taken into account is a quite simple way because it consists of intrasubband and intersubband terms which have clear physical meanings [29]

$$\gamma^{(a)}_{opt} = \gamma_{intra} + \gamma_{inter}, \qquad (22)$$

where $\gamma_{inter} = \nu_{2\to 1}/2$,

$$\gamma_{intra} = \frac{1}{2}\left(\nu_{1\leftrightarrow 1} + \nu_{2\leftrightarrow 2}\right) - \nu^{(coh)}_{1,2}, \qquad (23)$$

$\nu_{1\leftrightarrow 1}$ and $\nu_{2\leftrightarrow 2}$ represent usual intrasubband relaxation rates, and $\nu_{2\to 1}$ is the intersubband relaxation rate. The last term in Eq. (23), $\nu^{(coh)}_{1,2}$, has an unusual structure [29]

$$\nu_{1,2}^{(\mathrm{coh})} = \frac{2\pi}{\hbar}\sum_{s'}\left\langle (H_{\mathrm{int}})_{2,s;2s'}(H_{\mathrm{int}})_{1,s';1,s}\right\rangle \delta(\varepsilon_s - \varepsilon_{s'}) \qquad (24)$$

which guarantees the physical requirement that intra-subband linewidth contribution γ_{intra} should vanish in the case that the effective potentials of scatterers are the same for the both subbands $l = 2$ and $l = 1$ (the coherence of the initial superposition of two states is not perturbed by interaction with a scatterer [30]). Here $\langle ... \rangle$ means averaging over scatterers and ε_s represents the in-plane energy spectrum; in Ref. 29 the multi-component index s is just the 2D wave-vector $\mathbf{k}$. It should be noted that $\nu_{1,2}^{(\mathrm{coh})}$ has no relation to intersubband scattering because the energy conservation δ-function does not contain the intersubband excitation energy $\Delta_{2,1}$, and the matrix elements $(H_{\mathrm{int}})_{l,s;l's'} \equiv \equiv \langle l,s|H_{\mathrm{int}}|l',s'\rangle$ of different subbands enter Eq. (24) in an unusual way.

In order to find $\gamma_{\mathrm{opt}}^{(a)}$ for a quantizing magnetic field, we shall set $s = (n, X)$ and evaluate quantities $\overline{\nu}_{1\leftrightarrow 1}$ and $\overline{\nu}_{2\leftrightarrow 2}$ (averaged using the Boltzmann distribution) in the way used above for finding $\overline{\nu}_{l\to l'}^{(a)}$ of Eq. (4). Then, the proper expression for $\overline{\nu}_{1,2}^{(\mathrm{coh})}$ will be found from the condition of vanishing γ_{intra} if $p_{2,2} = p_{1,1} = p_{2,1}$. This procedure yields

$$\overline{\nu}_{l\leftrightarrow l}^{(a)} = \frac{\hbar\nu_0^{(a)}}{m_e S_{\mathrm{A}}} p_{l,l}\sum_{\mathbf{q}} S_{l,l}(q,0). \qquad (25)$$

We use the superscript (a) for quantities induced by vapor atoms. Equation (25) can also be found formally from Eq. (4) by fixing $l' = l$. The averaged value of $\nu_{2\to 1}^{(a)}$ coincides obviously with $\overline{\nu}_{2\to 1}^{(a)}$ defined by Eq. (4).

The averaged value of the specific term $\nu_{1,2}^{(\mathrm{coh})}$ can be represented as

$$\overline{\nu}_{1,2}^{(\mathrm{coh})} = \frac{\hbar\nu_0^{(a)}}{m_e S_{\mathrm{A}}} p_{1,2}\sum_{\mathbf{q}} S_{2,1}(q,0). \qquad (26)$$

Then, γ_{intra} vanishes if $p_{1,2} = p_{2,2} = p_{1,1}$. It should be noted that for $B = 0$ and short-range scatterers, the unusual term $\overline{\nu}_{1,2}^{(\mathrm{coh})}$ remarkably coincides with $\overline{\nu}_{2\to 1}^{(a)}$, and, therefore, it is partly compensated by $\overline{\gamma}_{\mathrm{inter}} = \overline{\nu}_{2\to 1}^{(a)}/2$. In the presence of the magnetic field, $\overline{\nu}_{1,2}^{(\mathrm{coh})}$ and $\overline{\nu}_{2\to 1}^{(a)}$ are completely different. The negative term $-\overline{\nu}_{1,2}^{(\mathrm{coh})}$ has smooth dependence on B, while $\overline{\nu}_{2\to 1}^{(a)}$ has sharp maxima at $B = B_m$ due to the presence of $\omega_{2,1}$ in the frequency argument of the DSF entering Eq. (4).

For highly correlated 2D electron liquid, one should keep the Coulomb broadening of the DSF, as described in Eqs. (10) and (11). This yields

$$\overline{\nu}_{l\leftrightarrow l}^{(a)} = \frac{\hbar\omega_c}{\sqrt{\pi}}\nu_0^{(a)} p_{l,l}\sum_n \frac{\mathrm{e}^{-\varepsilon_n/T_e}}{Z_{\|}}\int_0^\infty \frac{I_{n,n}^2(x_q)}{\sqrt{\Gamma_l^2 + x_q\Gamma_C^2}}dx_q. \qquad (27)$$

In the limiting case $\Gamma_C \to 0$, we can use the relationship $\int_0^\infty I_{n,n}^2(x_q)dx_q = 1$ and find that under a quantizing magnetic field $\overline{\gamma}_{l\leftrightarrow l}^{(a)}$ is increased by $\hbar\omega_c/\sqrt{\pi}\Gamma_l$ as compared to the result found for $B = 0$. In a similar way, we can represent

$$\overline{\nu}_{1,2}^{(\mathrm{coh})} = \frac{\hbar\omega_c}{\sqrt{\pi}}\nu_0^{(a)} p_{1,2}\sum_n \frac{\mathrm{e}^{-\varepsilon_n/T_e}}{Z_{\|}}\int_0^\infty \frac{I_{n,n}^2(x_q)}{\sqrt{\Gamma_{2,1}^2 + x_q\Gamma_C^2}}dx_q, \qquad (28)$$

where $\Gamma_{l,l'} = \sqrt{(\Gamma_l^2 + \Gamma_{l'}^2)/2}$. It is quite obvious that Eqs. (27) and (28) satisfy the condition of vanishing γ_{intra} for the same scattering amplitudes at the two subbands. Alternatively, in Eq. (28) instead of $\sqrt{\Gamma_{2,1}^2 + x_q\Gamma_C^2}$ one can use a harmonic mean of $\sqrt{\Gamma_1^2 + x_q\Gamma_C^2}$ and $\sqrt{\Gamma_2^2 + x_q\Gamma_C^2}$. Numerical calculations indicate that this change induces a reduction in γ_{intra} which is less than 1 %.

The dependence of MW excitation rate r_{mw} on the ratio $\omega_{2,1}/\omega_c(B)$ at the resonance ($\omega = \omega_{2,1}$) is shown in Fig. 3 near $B = B_5$ for different conditions. The result of the single-electron (SE) theory which takes into account the inhomogeneous broadening ($\gamma_{\mathrm{opt}} = \gamma_{\mathrm{inh}} + \overline{\gamma}_{\mathrm{opt}}^{(a)}$) is shown by the blue solid line. It has a minimum at $B = B_5$ caused by the intersubband component $\overline{\gamma}_{\mathrm{inter}} = \overline{\nu}_{2\to 1}/2$. In the many-electron (ME) treatment with $T_e = T$ (blue dashed line), correlations move the whole line r_{mw} up because the Cou-

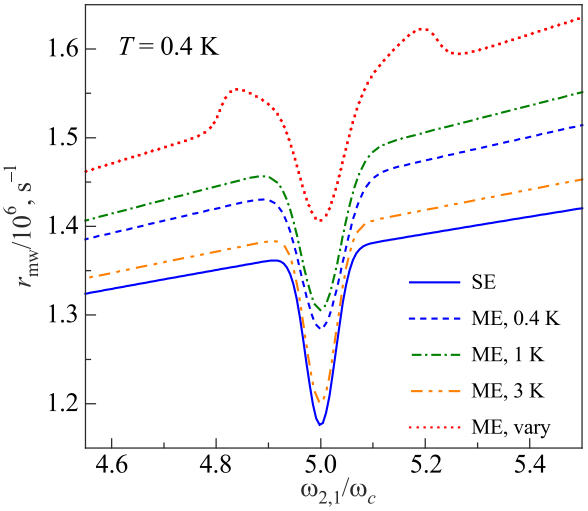

Fig. 3. (Color online) The excitation rate r_{mw} versus the ratio $\omega_{2,1}/\omega_c(B)$ calculated for $n_e = 2\cdot 10^6\,\mathrm{cm}^{-2}$, $\Omega_R = 10^8\,\mathrm{s}^{-1}$, and three fixed T_e: the single-electron theory (SE, blue solid), the many-electron theory (ME): $T_e = T$ (blue dashed), $T_e = 1\,\mathrm{K}$ (olive dash-doted), $T_e = 3\,\mathrm{K}$ (orange dash-dot-doted). The red dotted line was calculated for $n_e = 3\cdot 10^6\,\mathrm{cm}^{-2}$ and the solution $T_e(B)$ found below.

lomb broadening Γ_C reduces $\overline{\nu}^{(a)}_{l\leftrightarrow l}$, $\overline{\nu}^{(a)}_{1,2}$ and $\overline{\gamma}_{\rm inter}$ entering the denominator of Eq. (21). Medium heating up to $T_e = 1\,$K increases the ME effect ($E_f^{(0)} \propto \sqrt{T_e}$) as indicated by the olive dash-dotted line. Still, substantially stronger heating up to $T_e = 3\,$K (orange dash-dot-doted) moves the line down closer to the result of the SE theory because of the reduction in Γ_C described by Eq. (11) when the plasma parameter $\mathcal{P}_{\rm pl}$ becomes close to unity. In Fig. 3, we considered electron heating independent of B. In a real case, T_e is substantially higher at the vicinity of B_m than in regions where the staircases of Landau levels are out of alignment. This effect will be discussed in more details below, when considering resonant MW absorption. For other values of m, the MW excitation rate, as the function of $\omega_{2,1}/\omega_c(B)$, has similar shapes.

4. Energy relaxation

Energy dissipation in the multi-subband 2D electron system on liquid helium was described previously [12] only for noninteracting electrons. This method can be applied also to highly correlated electrons if we replace $S_{l,l'}(q,\Omega)$ with the ME form given in Eq. (10), and take into account some additional terms which become important for heated electrons. Therefore, for electron scattering by vapor atoms, we can find the normal contribution into energy dissipation of an electron per unit time proportional to $T_e - T$:

$$\dot{P}_N^{(a)} = -\left(T_e - T\right)\tilde{\nu}_N^{(a)}, \tag{29}$$

where

$$\tilde{\nu}_N^{(a)} = \frac{\hbar\varepsilon_R}{m_e T_e S_A}\sum_l \sum_{\mathbf{q}} \overline{n}_l \beta_{l,l} S_{l,l}\left(q,0\right) +$$

$$+\frac{\hbar\varepsilon_R}{m_e T_e S_A}\sum_{l>l'}\sum_{\mathbf{q}}\left(\overline{n}_l + \overline{n}_{l'}\mathrm{e}^{-\Delta_{l,l'}/T_e}\right)\beta_{l,l'} S_{l,l'}(q,\omega_{l,l'}) \tag{30}$$

is the normal energy relaxation rate of an electron caused by intrasubband (the first term) and intersubband (the second term) scattering, $\varepsilon_R = m_e\Lambda^2/2\hbar^2$ is the typical energy parameter of Rydberg states on liquid helium, $\beta_{l,l'} = \nu_0^{(a)}\lambda_{l,l'}(x)m_e/M$,

$$\lambda_{l,l'}\left(x\right) = u_{l,l'} + x\frac{\hbar\omega_c}{\varepsilon_R}\,p_{l,l'}, \tag{31}$$

$$u_{l,l'} = \frac{B_{1,1}}{\gamma_z^2 L_z}\sum_{k_z} k_z^2 \left|(\mathrm{e}^{ik_z z})_{l',l}\right|^2, \tag{32}$$

$\gamma_z^{-1} = \hbar^2/m_e\Lambda$ is the localization length of an electron in the ground Rydberg state, and M is the mass of a vapor atom. As expected, the energy relaxation rate $\tilde{\nu}_N^{(a)}$ is reduces as compared to the momentum relaxation rate by the mass ratio m_e/M which enters the parameter $\beta_{l,l'}$.

According to Eq. (30), $\tilde{\nu}_N^{(a)}$ is the sum of contributions from intrasubband and intersubband scattering: $\tilde{\nu}^{(a)}_{N,\rm intra}$ and $\tilde{\nu}^{(a)}_{N,\rm inter}$. Using the ME form of the DSF, one can find

$$\tilde{\nu}^{(a)}_{N,\rm intra} = \nu_0^{(a)}\frac{m_e}{M}\frac{\hbar\omega_c\varepsilon_R}{\sqrt{\pi}\Gamma_1 T_e}\sum_l \overline{n}_l\frac{\Gamma_1}{\Gamma_l}F_l^{(N)}\left(B\right), \tag{33}$$

where we introduced the dimensionless function

$$F_l^{(N)}\left(B\right) = \sum_n \frac{\mathrm{e}^{-\varepsilon_n/T_e}}{Z_\parallel}\int_0^\infty dx I_{n,n}^2(x)\frac{\lambda_{l,l}(x)\Gamma_l}{\sqrt{\Gamma_l^2 + x\Gamma_C^2}}. \tag{34}$$

Obviously, $F_l^{(N)}(B)$ is a smooth function. It should be noted here the presence of the enhancement factor $\hbar\omega_c/\sqrt{\pi}\Gamma_1$ mentioned above.

In a similar way, the contribution $\tilde{\nu}^{(a)}_{N,\rm inter}$ can be found as

$$\tilde{\nu}^{(a)}_{N,\rm inter} = \nu_0^{(a)}\frac{m_e}{M}\frac{\hbar\omega_c\varepsilon_R}{\sqrt{\pi}T_e\Gamma_{2;1}}\left(\overline{n}_2 + \overline{n}_1\mathrm{e}^{-\Delta_{2,1}/T_e}\right)F_{2,1}^{(N)}, \tag{35}$$

where

$$F_{2,1}^{(N)}\left(B\right) = \sum_{n=0}^{\infty}\frac{e^{-\varepsilon_n/T_e}}{Z_\parallel}\sum_{m=1}^{\infty}\frac{n!}{(n+m)!}\times$$

$$\times\int_0^\infty dx\lambda_{2,1}\left(x\right)\frac{\Gamma_{2;1}x^m\mathrm{e}^{-x}\left[L_n^m(x)\right]^2}{\sqrt{\Gamma_{2;1}^2 + x\Gamma_C^2}}\mathcal{G}_m\left(x\right), \tag{36}$$

and

$$\mathcal{G}_m\left(x\right) = \exp\left\{-\frac{\left[\Delta_{2,1} - m\hbar\omega_c - (\Gamma_2^2 + x\Gamma_C^2)/4T_e\right]^2}{\Gamma_{2;1}^2 + x\Gamma_C^2}\right\} \tag{37}$$

is the Gaussian factor entering the DSF. Thus, the normal contribution from intersubband scattering as a function of B represents rather sharp peaks placed at $B = B_m$ whose broadening is affected by the Coulombic effect due to $x\Gamma_C^2$.

In addition to the normal terms ($\dot{P}_N^{(a)}$) which vanish at $T_e \to T$, the average energy dissipated by an electron per unit time has the anomalous terms $\dot{P}_A^{(a)}$ which originate from the expansion of $S_{l,l'}(q,\omega_{l,l'} - \chi_{\mathbf{K},\mathbf{K}'})$ in $\chi_{\mathbf{K},\mathbf{K}'}$, where $\hbar\chi_{\mathbf{K},\mathbf{K}'}$ is the energy exchange at a collision. The anomalous terms can be represented as

$$\dot{P}_A^{(a)} = \frac{2T\varepsilon_R}{m_e S_A}\sum_{l>l'}\sum_{\mathbf{q}}\left(\overline{n}_l - \overline{n}_{l'}\mathrm{e}^{-\Delta_{l,l'}/T_e}\right)\beta_{l,l'}\times$$

$$\times\left[S'_{l,l'}(q,\omega_{l,l'}) - \frac{\hbar}{2T_e}S_{l,l'}(q,\omega_{l,l'})\right], \tag{38}$$

where the prime superscript of $S'_{l,l'}$ means the derivative with respect to the frequency argument. Using the ME form of the DSF one can find

$$\dot{P}_A^{(a)} = -\nu_0^{(a)} \frac{m_e}{M}\left(\overline{n}_2 - \overline{n}_1 \mathrm{e}^{-\Delta_{2,1}/T_e}\right)\frac{4\hbar\omega_c T\varepsilon_R}{\sqrt{\pi}\Gamma_{2;1}^2} F_{2,1}^{(A)}, \qquad (39)$$

where we introduced a new dimensionless function

$$F_{2,1}^{(A)} = \sum_{n=0}^{\infty}\frac{\mathrm{e}^{-\varepsilon_n/T_e}}{Z_{\|}}\sum_{m=1}^{\infty}\frac{n!}{(n+m)!}\int_0^{\infty} dx\lambda_{2,1}(x)x^m\mathrm{e}^{-x}\times$$

$$\times\left[L_n^m(x)\right]^2\Gamma_{2;1}^2\frac{(\hbar\omega_{2,1}-m\hbar\omega_c)}{(\Gamma_{2;1}^2+x\Gamma_C^2)^{3/2}}\mathcal{G}_m(x). \qquad (40)$$

In the round brackets of the integrand of Eq. (40) we have neglected the quantity $(\Gamma_1^2-\Gamma_2^2)/8T_e$ which is more than two orders of magnitude smaller than Γ_1.

As compared to the normal contribution from intersubband scattering, $\dot{P}_A^{(a)}$ contains an additional large parameter $4T/\Gamma_{2;1}$ which compensates a possible smallness of $\overline{n}_2 - \overline{n}_1\mathrm{e}^{-\Delta_{2,1}/T_e}$. The anomalous function $F_{2,1}^{(A)}(B)$ has a sign-changing shape which resembles the derivative of series of maxima. Its difference from $F_{2,1}^{(N)}(B)$ is illustrated in Fig. 4. Under certain conditions the energy dissipation caused by electron interaction with medium can be negative which leads to additional heating of electrons. In contrast to the momentum relaxation rate [12, 15], the minima of $\dot{P}_A$ occur at the opposite side with respect to the points $B = B_m$ where $\omega_{2,1}/\omega_c$ is a bit less than m.

At low temperatures $T \lesssim 0.4$ K, one cannot disregard energy relaxation caused by 2R processes because the energy exchange $2\hbar\omega_q$ can be rather high for short-wavelength ripplons. The contribution of these processes into the energy dissipation per unit time can be calculated in a direct way using the lowest Born approximation for the interaction Hamiltonian given in Eq. (12). For example, 2R emission leads to

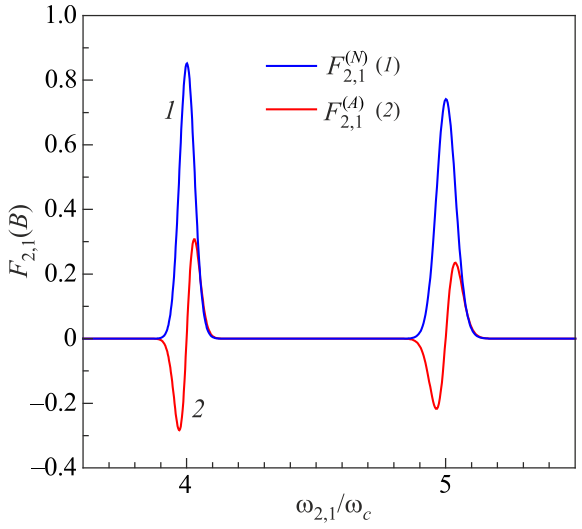

Fig. 4. (Color online) Two functions $F_{2,1}^{(N)}$ and $F_{2,1}^{(A)}$ describing energy relaxation for intersubband scattering versus the ratio $\omega_{2,1}/\omega_c(B)$.

$$\dot{P}_{2\mathrm{R}}^{(\mathrm{em})} = -\frac{\hbar^2}{\rho^2\ell_B^2 S_A}\sum_{l,l'}\overline{n}_l\sum_{n,n'}\frac{\mathrm{e}^{-\varepsilon_n/T_e}}{Z_{\|}}\sum_{\mathbf{q}}\left(W_q\right)_{l',l}^2\frac{q^2}{\omega_q}\times$$

$$\times\left(N_q+1\right)^2\delta\left(\varepsilon_{n'}-\varepsilon_n-\Delta_{l,l'}+2\hbar\omega_q\right). \qquad (41)$$

The contribution from 2R absorption $\dot{P}_{2\mathrm{R}}^{(\mathrm{ab})}$ has a similar form: one have to replace $\mathcal{N}_q+1$ with $\mathcal{N}_q$, change $+2\hbar\omega_q$ to $-2\hbar\omega_q$ and change the sign of the whole expression.

By interchanging the summation indexes, the full contribution of 2R processes $\dot{P}_{2\mathrm{R}} = \dot{P}_{2\mathrm{R}}^{(\mathrm{em})} + \dot{P}_{2\mathrm{R}}^{(\mathrm{ab})}$ can be represented as

$$\dot{P}_{2\mathrm{R}} = -\frac{\hbar}{4\pi\rho^2\ell_B^2}\sum_{n,n'}\frac{\mathrm{e}^{-\varepsilon_n/T_e}}{Z_{\|}}\sum_{l,l'}\left\{Y_{l,l'}(q)\right\}_{q=q_m^{(l,l')}}, \qquad (42)$$

where $m = n'-n$,

$$q_m^{(l,l')} = \left(\frac{\rho}{4\alpha}\right)^{1/3}\left(\omega_{l,l'}-m\omega_c\right)^{2/3}\theta\left(\omega_{l,l'}-m\omega_c\right), \qquad (43)$$

$$Y_{l,l'}(q) = \left(W_q\right)_{l',l}^2\frac{q^3}{\omega_q\left|\omega_q'\right|}\left(\mathcal{N}_q+1\right)^2\times$$

$$\times\left\{\overline{n}_l - \overline{n}_{l'}\mathrm{e}^{-\Delta_{l,l'}/T_e}\exp\left[-2\hbar\omega_q\frac{(T_e-T)}{T_eT}\right]\right\}, \qquad (44)$$

and ω_q' is the derivative of the ripplon spectrum. In contrast to the decay rate, Eq. (42) contains also the contribution from intrasubband scattering ($l = l'$). In the limiting case $T_e \to T$, it is proportional to $T_e - T$. At medium heating, the parameter entering the exponential function of Eq. (44) is not small and the dependence on T_e complicates. From Eq. (44) one can see that at equilibrium ($T_e = T$, and $\overline{n}_l = \overline{n}_{l'}\mathrm{e}^{-\Delta_{l,l'}/T_e}$) the dissipation $\dot{P}_{2\mathrm{R}} = 0$. It should be noted also that for nonequilibrium population of the excited subband $\overline{n}_2 - \overline{n}_1\mathrm{e}^{-\Delta_{2,1}/T_e} > 0$, the contribution $\dot{P}_{2\mathrm{R}} \neq 0$ even if $T_e = T$.

Electron temperature is obtained by balancing the power taken from the field $\dot{P}_{\mathrm{mw}} = (\overline{n}_1 - \overline{n}_2)\Delta_{2,1}r_{\mathrm{mw}}$ and the power transferred to vapor atoms and ripplons

$$\dot{P}_{\mathrm{mw}} + \dot{P}_N^{(a)} + \dot{P}_A^{(a)} + \dot{P}_{2\mathrm{R}} = 0. \qquad (45)$$

Solutions of Eq. (45) are shown in Fig. 5 as functions of B near the point B_5 for different physical models. The single-electron (SE) approximation for $T_e(B)$ which does not include 2R processes (dotted black line *1*) represents an asymmetric two-hump peak. The local minimum is placed very close to B_5. In regions $B < 0.77$ T and $B > 0.81$ T the electron temperature practically coincides with T. For the SE theory which takes into account the 2R processes, the two-hump peak is substantially lower and there is electron heating in regions where B differs strongly from B_5. In spite of a rather low electron density chosen for these cal-

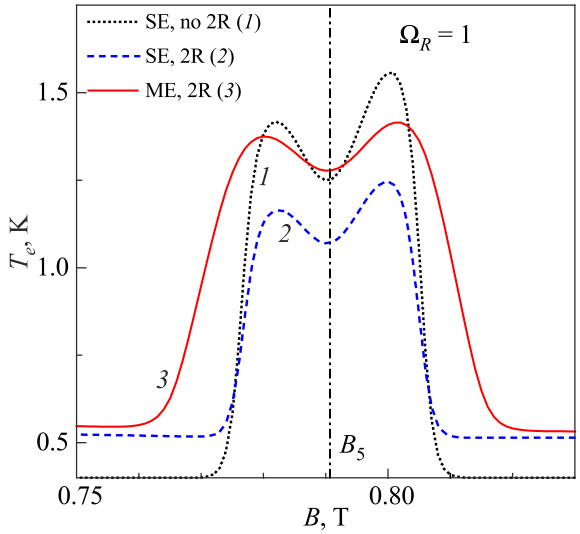

Fig. 5. (Color online) The electron temperature versus B in the vicinity of B_5 calculated using different approximations: the SE theory disregarding 2R scattering [black doted (*1*)], the SE theory taking into account 2R scattering [blue dashed (*2*)], the ME theory for $n_e = 2\cdot10^6\,\mathrm{cm}^{-2}$ [red (*3*)]. The Rabi frequency Ω_R is given in units of $10^8\,\mathrm{s}^{-1}$.

culations ($n_e = 2\cdot10^6\,\mathrm{cm}^{-2}$), the ME treatment given in this work changes the two-hump peak of $T_e(B)$ strongly, as indicated by the solid red line. The peak becomes broader especially in regions of tails, and the asymmetry of two humps is reduced.

The dependence of the electron temperature peak on n_e caused by the ME effect with Γ_C defined by Eq. (11) is illustrated in Fig. 6. The lowest line [black (*1*)] represents the result of the SE theory. Other lines were calculated using the ME theory with electron density gradually increased from $n_e = 2\cdot10^6\,\mathrm{cm}^{-2}$ [blue line (*2*)] up to $n_e = 5\cdot10^6\,\mathrm{cm}^{-2}$ [red line (5)]. One can see that the ME effect increases electron temperature because main relaxation rates are reduced by the Coulomb broadening Γ_C while the MW excitation rate $r_{\mathrm{mw}} \propto 1/\gamma_{\mathrm{opt}}$ rises. Another important point is that electron Coulomb interaction changes the asymmetry of the two-hump peak of $T_e(B)$ to the opposite [red (5) and orange (4)] as compared to the result of the SE theory [12]. The right maximum with $\omega_{2,1}/\omega_c > 5$ becomes higher that the left maximum ($\omega_{2,1}/\omega_c < 5$). Thus, the asymmetry of the T_e peaks becomes the same as the asymmetry of power absorption [19]. The difference in asymmetries of electron temperature peaks in the SE theory [12] and MW absorption peaks observed was stated [19] to be an important point in discussions about the origin of the effect. Actually, as we shall see below, the correct asymmetry of the MW absorption ($\dot{P}_{\mathrm{mw}}$) peaks appears already in the SE treatment and it does not correlate with the asymmetry of the electron temperature peaks.

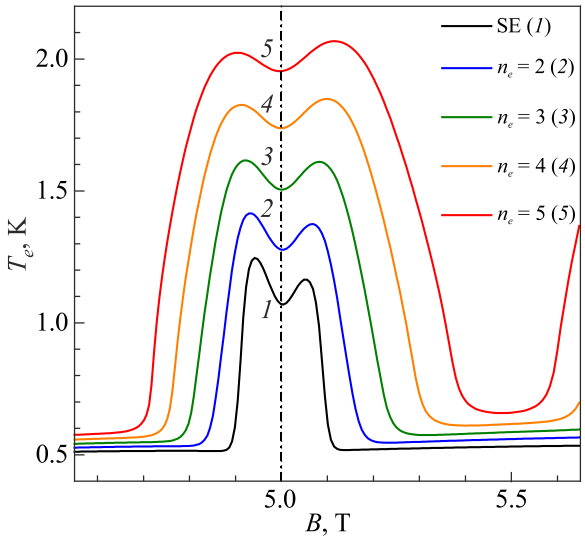

Fig. 6. (Color online) Electron temperature versus the ratio $\omega_{2,1}/\omega_c(B)$ for different n_e shown in the figure legend in units of $10^6\,\mathrm{cm}^{-2}$. The Rabi frequency $\Omega_R = 10^8\,\mathrm{s}^{-1}$ and $T = 0.4$ K.

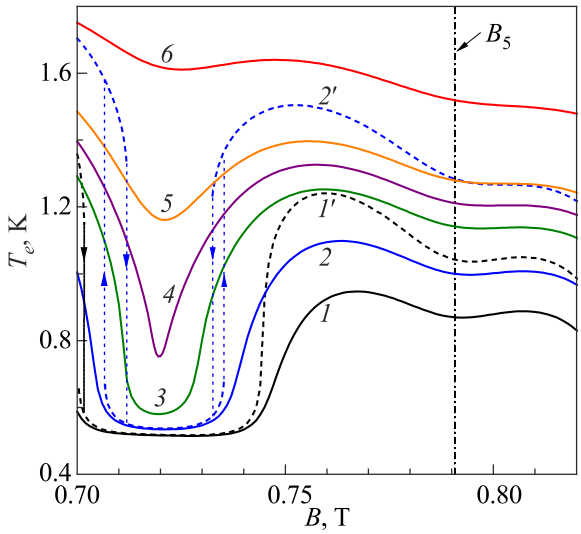

Fig. 7. (Color online) Electron temperature versus B for different models of the ME effect in the region where the B_5 peak mixes with the B_6 peak: the approximation $\Gamma_C = \Gamma_f$ (dashed lines), the interpolation of Eq. (11) (solid lines). Calculations are performed for different densities (given in units of $10^6\,\mathrm{cm}^{-2}$): $n_e = 5$ [black lines (*1*) and (*1′*)], 6 [blue lines (*2*) and (*2′*)], 7 [olive (*3*)], 7.5 [purple (*4*)], 8 [orange (*5*)] and 10 [red (*6*)].

It is interesting to compare the results of the new ME electron treatment given above with the approximation $\Gamma_C = \Gamma_f$ which does not take into account the reduction of the Coulomb broadening at $\mathcal{P}_{\mathrm{pl}} < 10$ described by Eq. (11). The qualitative differences appear in regions of peak tails especially when temperature peaks of different B_m start overlapping. This situation is illustrated in Fig. 7 where the ME effect on electron heating near B_5 mixes with the same effect near B_6. The results of the theory based on the approximation $\Gamma_C = \Gamma_f$ are shown by dashed lines calculated for medium excitation ($\Omega_R = 6.25\cdot10^7\,\mathrm{s}^{-1}$) and two electron densities: $n_e = 5\cdot10^6\,\mathrm{cm}^{-2}$ [black (*1′*)] and

$n_e = 6\cdot10^6\,\mathrm{cm}^{-2}$ [blue (*2′*)]. One can see that the blue dashed line has two regions of temperature bistability which would lead to specific hysteresis phenomena. For example, at higher densities (not shown in this figure) the high-temperature branches touch each other and merge becoming a single branch, while the low temperature branch remains and it becomes a non-reentrant branch: the system can jump vertically to the high-temperature branch, but cannot return back to the low-temperature branch. The theory which takes into account the reduction of Γ_C caused by electron heating (solid lines) eliminates this puzzling effect: the overlapping of two temperature peaks is continuous, and the non-reentrant branch does not appear.

5. MW absorption

Experimental study [19] of intersubband absorption in electrons on liquid helium under quantizing magnetic fields revealed an unexpected feature: the strong suppression of absorption at magnetic fields where $B \to B_m$. It is tempting to attribute this effect to electron temperature minima caused by the correction $\overline{\gamma}_{\mathrm{inter}} = \overline{\nu}^{(a)}_{2\to1}/2$ to the linewidth γ_{opt}. Still, as noted in Ref. 19, the asymmetry of the two-hump peaks of intersubband absorption observed was opposite to the asymmetry of electron temperature peaks obtained in the SE theory [12]. This seeming discrepancy between the theory and experiment is caused by the assumption that MW power absorption is an increasing function of electron temperature, as it is for usual intrasubband absorption, and a higher electron temperature should correspond to higher MW absorption. We would like to emphasize here that for intersubband excitation this is not true because intersubband MW absorption mostly increases the potential energy of electrons and have no direct relation to an increase in the in-plane kinetic energy. The kinetic energy of electrons increases due to decay scattering process, and, therefore, the relationship between T_e and intersubband MW absorption can be even opposite. In order to eliminate this seeming discrepancy consider MW absorption per an electron $\dot{P}_{\mathrm{mw}}$ in more details.

It is instructive to plot $\dot{P}_{\mathrm{mw}} = (\overline{n}_1 - \overline{n}_2)\Delta_{2,1} r_{\mathrm{mw}}$ versus the electron temperature, as shown in Fig. 8. Calculations were performed using the ME theory (solid lines) and the SE approximation (dashed lines) for three characteristic values of the magnetic field: $B_5 = 0.79\,\mathrm{T}$, $B_L = 0.78\,\mathrm{T}$, and $B_R = 0.802\,\mathrm{T}$, where B_L and B_R correspond to the local maxima of $T_e(B)$. In the SE theory, the decay rate ($\overline{\nu}_{2\to1}$), linewidth (γ_{opt}) and MW excitation rate (r_{mw}) are independent of the electron temperature. Therefore, the dependence $\dot{P}_{\mathrm{mw}}(T_e)$ is caused only by the respective dependence of $\overline{n}_1 - \overline{n}_2$. In the vicinity of B_m, 2R decay processes can be disregarded even in the expression for the relative occupancy $\eta = \overline{n}_2/\overline{n}_1$ defined by Eq. (20). As a result, the electron temperature enters η and the difference

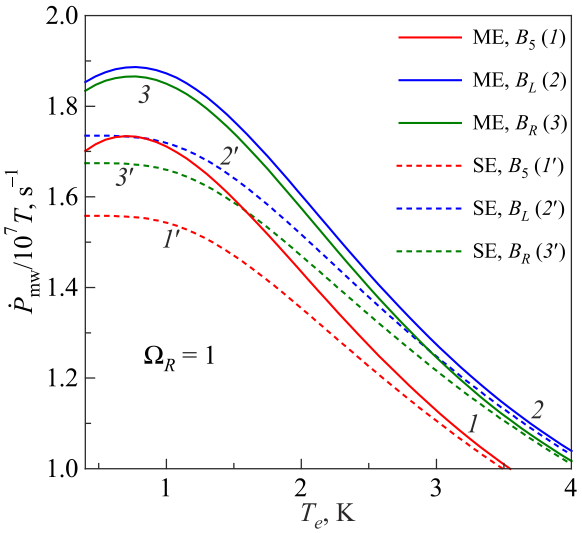

Fig. 8. (Color online) MW power absorbtion $\dot{P}_{\mathrm{mw}}$ versus T_e calculated for three characteristic values of the magnetic field: $B_5 = 0.79\,\mathrm{T}$ [red lines (*1*) and (*1′*)], $B_L = 0.78\,\mathrm{T}$ [blue lines (*2*) and (*2′*)], and $B_R = 0.802\,\mathrm{T}$ [olive lines (*3*) and (*3′*)]. The single-electron approximation is shown by dashed lines, the ME theory ($n_e = 2\cdot10^6\,\mathrm{cm}^{-2}$) — solid lines. Ω_R is given in units of $10^8\,\mathrm{s}^{-1}$.

$\overline{n}_1 - \overline{n}_2$ only by means of the reverse scattering term $\overline{\nu}^{(a)}_{2\to1} e^{-\Delta_{2,1}/T_e}$. At low T_e, it is exponentially small, and, therefore, $\dot{P}_{\mathrm{mw}}$ is practically independent of the electron temperature, as illustrated in Fig. 8. Even in this regime, where $\dot{P}_{\mathrm{mw}}(T_e) \approx \mathrm{const}$, MW absorption is proportional to r_{mw} which has a sharp dip at $B = B_m$ shown in Fig. 3. Therefore, the two-hump shape of $\dot{P}_{\mathrm{mw}}(B)$ appears independently of T_e: according to Fig. 8, intersubband absorption at B_5 (red dashed) is substantially lower than at B_L and B_R. Moreover, the higher dashed line corresponds to the lower field B_L which is in contrast with the two-hump line of $T_e(B)$, and in accordance with the experimental observations [19].

Further increase in T_e (above 1 K) obviously depletes the population of the ground subband (the relative ocupancy η increases) and reduces $\dot{P}_{\mathrm{mw}}$. Numerical calculations shown in Fig. 8 confirm this conclusion. Thus, in the SE theory the intersubband absorption decreases with T_e which is in contrast with the usual picture of intrasubband absorption. The solid lines calculated using the ME theory show a small maximum at $T_e \simeq 0.73\,\mathrm{K}$, nevertheless, this effect does not change the vertical order of these lines: it remains the same as for the dashed lines.

The dependence $\dot{P}_{\mathrm{mw}}(\omega_{2,1}/\omega_c)$ near the point $m = 5$ is illustrates in Fig. 9 for five densities: the lowest solid line represents the SE theory ($n_e \to 0$), and for other lines electron density shown in units of $10^6\,\mathrm{cm}^{-2}$ gradually changes from $n_e = 2$ [olive line (*3*)] to $n_e = 5$ [red line (*5*)]. Even though the positions of $\dot{P}_{\mathrm{mw}}(\omega_{2,1}/\omega_c)$ maxima and

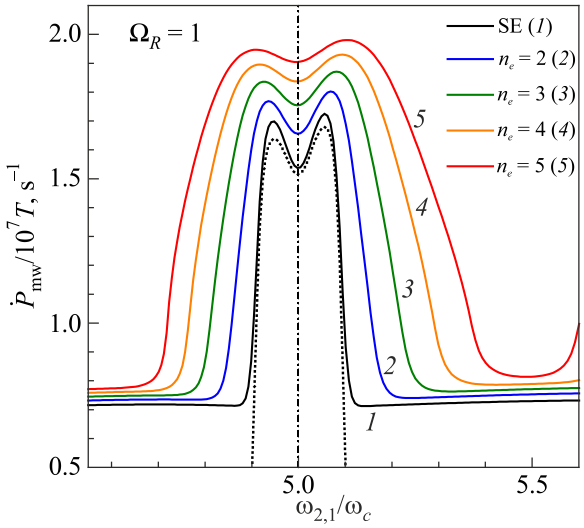

Fig. 9. (Color online) MW power absorbtion $\dot{P}_{mw}$ versus the ratio $\omega_{2,1}/\omega_c$ calculated for different n_e shown in the figure legend in units of $10^6\,cm^{-2}$. The black dotted line represents the SE theory which disregards the 2R scattering.

$T_e(\omega_{2,1}/\omega_c)$ maxima are remarkably very close, the asymmetry of the two-hump line $\dot{P}_{mw}(\omega_{2,1}/\omega_c)$ calculated for $n_e \to 0$ (SE) is opposite to the asymmetry of the respective line of $T_e(\omega_{2,1}/\omega_c)$ shown in Fig. 6. It should be noted also that the ME effect does not change the asymmetry of power absorption peaks which is in contrast with electron temperature peaks.

The suppression of $\dot{P}_{mw}$ at $\omega_{2,1}/\omega_c = m$ becomes stronger for lower excitation rates (or lower Ω_R), as illustrated in Fig. 10 and in its insert. Here, the solid lines represent the SE theory and the dotted line represents the ME theory for $n_e = 3\cdot10^6\,cm^{-2}$. Remarkably, at low Ω_R the

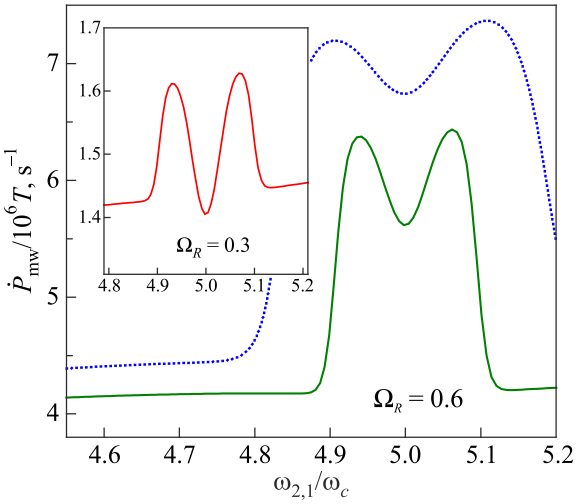

Fig. 10. (Color online) The MW absorption two-hump peak calculated for two Rabi frequencies Ω_R shown in units of $10^8\,s^{-1}$. Solid lines represent the single-electron theory. The dashed line is calculated for $n_e = 3\cdot10^6\,cm^{-2}$ using the ME theory described in the text.

minimum of the SE line can be even deeper than the tails of $\dot{P}_{mw}(\omega_{2,1}/\omega_c)$.

The factor $(\bar{n}_1 - \bar{n}_2)$ entering the definition of $\dot{P}_{mw}(\omega_{2,1}/\omega_c)$ has a form of a single maximum positioned at $\omega_{2,1}/\omega_c = m$. Therefore, the two-hump structure of $\dot{P}_{mw}(\omega_{2,1}/\omega_c)$ originates from the dependence $r_{mw}(\omega_{2,1}/\omega_c)$ illustrated in Fig. 3. In this figure, the result of the ME theory evaluated for $n_e = 3\cdot10^6\,cm^{-2}$ and for actual dependence $T_e(B)$ is shown by the red dotted line. Besides the minimum caused by $\bar{\gamma}_{inter} = \bar{\nu}^{(a)}_{2\to1}/2$, this line has also two-hump maxima originated from $\bar{\gamma}_{inter}(T_e)$ which has a non-monotonic dependence on electron temperature. It decreases strongly at first due to the Coulomb broadening $\Gamma_C(T_e)$, then attains a minimum at $T_e \approx 1\,K$, and then starts increasing because electron heating reduces the plasma parameter $\mathcal{P}_{pl}$ entering Eq. (11) and increases population of higher Landau levels.

6. Discussion and conclusion

The theoretical analysis presented here indicates that in a nonequilibrium multisubband 2D electron system under a quantizing magnetic field, even without a well defined Fermi level (nondegenerate gas), nearly all its basis quantities should have $1/B$-periodic oscillations caused by squeezing of the density of states into sharp Landau levels. We have shown that, besides the DC magnetoconductivity, such oscillatory features are present in the energy relaxation rate, the intersubband-resonance linewidth, electron temperature, subband occupancies, and MW power absorption. These kind of oscillations obtain an unusual shape when the displacement from equilibrium distribution cannot be reduced to trivial heating. Such a condition is realized when the electron system is tuned into the resonance with the MW field whose polarization vector has a perpendicular component. For example, in this case the energy relaxation rate as a function of B has asymmetrical sign-changing corrections which leads to a distinctive asymmetry of electron temperature peaks with respect to special points B_m, where the staircases of Landau levels of the ground subband and an excited subband become aligned.

Strong heating of surface electrons on liquid helium occurs in the vicinity of the special points B_m because of the interplay of MW resonance absorption ($\omega = \Delta_{2,1}/\hbar$) and the quasi-elastic electron decay to the ground subband. This kind of scattering cannot transfer the intersubband excitation energy $\Delta_{2,1}$ directly to a vapor atom or to a ripplon because of momentum conservation, but it can transfer it to the kinetic energy of electrons which heats the system. At the same time, inelastic emission of a par of energetic ripplons with a small total momentum which occurs at any magnetic field leads to small or medium heating of electrons even if the staircases of Landau levels are out of alinement. The two-hump shape of the electron peak near B_m appears because of magnetooscillations of the linewidth of the intersubband resonance $\gamma^{(a)}_{opt}$. The

linewidth has sharp maxima at the points $B = B_m$ which is the reason for deep minima of the MW excitation rate $r_{\rm mw} \propto 1/\gamma_{\rm opt}^{(a)}$ under the resonant condition.

As noted above, a two-hump peak of electron temperature have the distinctive asymmetry with respect to the point B_m shown in Fig. 5: at low electron densities, the maximum which is placed at $B > B_m$ is higher than another one placed at $B < B_m$. Previously, it was assumed [19] that the asymmetry of the power absorption peaks should be the same as the asymmetry of electron temperature peaks, and the different asymmetry observed for intersubband absorption was a main reason for the conclusion that the linewidth maxima are not responsible for this effect. In this work, we have demonstrated that MW power absorption has a complicated and nontrivial dependence on electron temperature indicated in Fig. 8, which differs qualitatively from the respective dependence of intrasubband absorption. For example, at low n_e and T_e, intersubband absorption is nearly independent of T_e, while at higher electron temperatures $T_e > 1$ K it even decreases. Nevertheless, as a function of B it has two-hump peaks with an asymmetry which is opposite to the asymmetry of electron temperature peaks which agrees with experimental observations. The depth of the power absorption dip at $B = B_m$ depends on the Rabi frequency Ω_R. As indicated in Fig. 10, a moderate reduction in Ω_R can make the minimum deeper with regard to the region of tails.

The many-electron effect is shown to play an important role in a 2D electron system subjected to a perpendicular magnetic field. It increases the Coulomb broadening Γ_C of the DSF of the electron liquid and, therefore, reduces electron relaxation rates. This leads to heating of the electron system. In turn, heating influences the ME effect in a nontrivial way. First, it increases the ME effect because the internal electric field E_f of fluctuational origin is proportional to $T_e^{1/2}$. Then, at higher T_e and a fixed electron density, the kinetic energy of electrons increases and the system approaches the regime where it can be described as noninteracting particles. In present work, this influence is taken into account by employing an interpolation form for Γ_C as a function of the plasma parameter. Remarkably, the Coulombic effect is shown to invert eventually the asymmetry of electron temperature peaks, but it does not affect the asymmetry of power absorption peaks. An increase in electron density n_e broadens the $\dot{P}_{\rm mw}$ peaks due to the ME effect and reduces the dips at $B = B_m$ which also agrees with observations [19].

At high enough electron densities, the model based on the approximation $\Gamma_C = \Gamma_f \propto T_e^{1/2}$ leads to existence of bistability regions placed at tails of a temperature peak. In this case, overlapping of electron temperature peaks which belong to nearest B_m becomes discontinuous and can cause puzzling non-reentrant states. The new model taking into account the reduction of Γ_C induced by strong heating of electrons eliminates the bistability regions at least for the vapor atom scattering regime. For the ripplon scattering regime which is not considered in this work, the ambient temperature is substantially lower $T \le 0.2$ K and the approximation $\Gamma_C = \Gamma_f \propto T_e^{1/2}$ can be valid in a broader range of T_e. Therefore, there is a chance that the hysteresis observed [20] for $\sigma_{xx}(B)$ is caused by the electron temperature bistability.

In this work, we had restricted our consideration mostly to the vapor atom scattering regime, though electron scattering with pairs of energetic ripplons was also taken into account. The numerical calculations were performed for liquid ^{3}He with the fixed temperature $T = 0.4$ K which was quite close to the temperature used in the ripplon dominated experiment ($T = 0.2$ K). Since the electron interaction with long-wavelength ripplons is not that simple as the electron-atom interaction, and it leads to certain complications in numerical evaluations, the theory presented here can be considered also as a model for qualitative understanding of the effects observed in the ripplon dominated regime.

The most important difference which appears at $T = 0.2$ K is that the inhomogeneous broadening $\gamma_{\rm inh}$ in the experiments [10, 19] is about one order of magnitude larger than $\gamma_{\rm intra}$ defined by one-ripplon scattering and five times larger than the maximum value of $\gamma_{\rm inter}$. It was assumed [19] that such a large value of $\gamma_{\rm inh}$ was caused by inhomogeneity of $E_\perp$ along the surface, and only a small part of electrons (about 10 %) was under condition of real intersubband resonance with $\gamma_{\rm opt}$ defined by electron-ripplon scattering. If this picture is true, then only a small part of electrons is strongly excited by the MW, but a large fraction of detuned electrons (about 90 %) contributes to energy relaxation because of electron correlations. This explains why electron temperature is not very high in these experiments (it is estimated to be about 1 K) in spite of strong excitation. On the other hand, the contribution into power absorbtion, which is proportional to $r_{\rm mw} \propto 1/\gamma_{\rm opt}$, from electrons with small $\gamma_{\rm opt} \sim \gamma_{\rm intra}$ can obviously be comparable or even larger than contribution from other electrons. Therefore, the reduction of $r_{\rm mw}$ caused by the sharp increase in $\overline{\gamma}_{\rm inter} = \overline{\nu}_{2\to1}^{(a)}/2$ can be the reason for the dips observed at $B = B_m$ when the staircases of Landau levels belonging to the ground subband and the excited subband become aligned. The detailed analysis of the ripplon dominated regime will be given elsewhere.

1. M. A. Zudov, R. R. Du, J. A. Simmons, and J. R. Reno, *Phys. Rev. B* **64**, 201311(R) (2001).
2. P. D. Ye, L. W. Engel, D. C. Tsui, J. A. Simmons, J. R. Wendt, G. A. Vawter, and J. L. Reno, *Appl. Phys. Lett.* **79**, 2193 (2001).
3. R. Mani, J. H. Smet, K. von Klitzing, V. Narayanamurti, W. B. Johnson, and V. Umansky, *Nature* **420**, 646 (2002).
4. M. A. Zudov, R. R. Du, L. N. Pfeiffer, and K. W. West, *Phys. Rev. Lett.* **90**, 046807 (2003).

5. M. A. Zudov, O. A. Mironov, Q. A. Ebner, P. D. Martin, Q. Shi, and D. R. Leadley, *Phys. Rev. B* **89**, 125401 (2014).
6. R. Yamashiro, L. V. Abdurakhimov, A. O. Badrutdinov, Yu. P. Monarkha, and D. Konstantinov, *Phys. Rev. Lett.* **115**, 256802 (2015).
7. D. F. Karcher, A. V. Shchepetilnikov, Yu. A. Nefyodov, J. Falson, I. A. Dmitriev, Y. Kozuka, D. Maryenko, A. Tsukazaki, S. I. Dorozhkin, I.V. Kukushkin, M. Kawasaki, and J. H. Smet, *Phys. Rev. B* **93**, 041410(R) (2016).
8. I. A. Dmitriev, A. D. Mirlin, D. G. Polyakov, and M. A. Zudov, *Rev. Mod. Phys*. **84**, 1709 (2012).
9. D. Konstantinov and K. Kono, *Phys. Rev. Lett.* **103**, 266808 (2009).
10. D. Konstantinov and K. Kono, *Phys. Rev. Lett*. **105**, 226801 (2010).
11. Yu. P. Monarkha, *Fiz. Nizk. Temp*. **37**, 108 (2011) [*Low Temp. Phys*. **37**, 90 (2011)].
12. Yu. P. Monarkha, *Fiz. Nizk. Temp*. **37**, 829 (2011) [*Low Temp. Phys.* **37**, 655 (2011)].
13. Yu. P. Monarkha, *Fiz. Nizk. Temp*. **46**, 682 (2020) [*Low Temp. Phys.* **46**, 569 (2020)].
14. D. Konstantinov, H. Isshiki, Yu. P. Monarkha, H. Akimoto, K. Shirahama, and K. Kono, *Phys. Rev. Lett*. **98**, 235302 (2007).
15. Yu. P. Monarkha, *Fiz. Nizk. Temp*. **38**, 579 (2012) [*Low Temp. Phys.* **38**, 451 (2012)].
16. Yu. P. Monarkha, *Fiz. Nizk. Temp*. **42**, 567 (2016) [*Low Temp. Phys*. **42**, 441 (2016)].
17. Yu. Monarkha and D. Konstantinov, *J. Low Temp. Phys*. **197**, 208 (2019).
18. D. Konstantinov, Yu. Monarkha, and K. Kono, *Phys. Rev. Lett*. **111**, 266802 (2013).
19. D. Konstantinov and K. Kono, *J. Phys. Soc. Jpn*. **82**, 043601 (2013).
20. D. Konstantinov, A. Chepelianskii, and K. Kono, *J. Phys. Soc. Jpn*. **81**, 093601 (2012).
21. M. I. Dykman and L. S. Khazan, *Zh. Eksp. Teor. Fiz.* **77**, 1488 (1979) [*Sov. Phys. JETP* **50**, 747 (1979)].
22. Yu. P. Monarkha, E. Teske, and P. Wyder, *Phys. Rep*. **370**, 1 (2002).
23. Yu.P. Monarkha and K. Kono, *Two-Dimensional Coulomb Liquids and Solids*, Springer-Verlag, Berlin, Heildelberg (2004).
24. Yu. P. Monarkha, *Fiz. Nizk. Temp*. **4**, 1093 (1978) [*Sov. J. Low Temp. Phys.* **4**, 515 (1978)].
25. Yu. P. Monarkha, S. S. Sokolov, A. V. Smorodin, and N. Studart, *Fiz. Nizk. Temp*. **36**, 711 (2010) [*Low Temp. Phys.* **36**, 565 (2010)].
26. T. Ando and Y. Uemura, *J. Phys. Soc. Jpn*. **36**, 959 (1974).
27. R. R. Gerhardts, *Surf. Sci*. **58**, 227 (1976).
28. E. Kawakami, A. Elarabi, and D. Konstantinov (arXiv:2009.11502v2).
29. T. Ando, *J. Phys. Soc. Jpn*. **44**, 765 (1978).
30. C. C. Grimes, T. R. Brown, M. L. Burns, and C. L. Zipfel, *Phys. Rev. B* **13**, 140 (1976).

Магнетоосциляції температури та поглинання мікрохвильового випромінювання в сильно корельованому двовимірному електронному газі над рідким гелієм

Yu. P. Monarkha

Теоретично досліджується вплив кулонівської взаємодії у двовимірному електронному газі над рідким гелієм на розігрівання електронів, що індукується мікрохвильовим випромінюванням за наявності квантуючого магнітного поля. Запропоновано узагальнення теорії ширини міжпідзонного резонансу, яке враховує як стискування щільності станів електронів у рівнях Ландау, так і наявність сильного внутрішнього електричного поля флуктуаційної природи. Ця теорія описує появу двогорбих піків електронної температури та поглинання мікрохвиль при певних значеннях напруженості магнітного поля. Показано, що при низьких концентраціях електронів асиметрія двогорбих піків мікрохвильового поглинання протилежна до асиметрії температурних піків, що пояснює результати експериментальних спостережень. Продемонстрована важливість процесів випромінювання пар короткохвильових ріплонів для опису заселеності електронних підзон та швидкості енергетичної релаксації.

Ключові слова: двовимірний електронний газ, магнетоосциляції, явища нерівноваги, міжпіддіапазонне мікрохвильове поглинання.